Architecture of Metaphase Chromosomes and Chromosome Scaffolds

WILLIAM C. EARNSHAW and ULRICH K. LAEMMLI

Departments of Molecular Biology and Biochemistry, University of Geneva, CH-1211 Geneva 4, Switzerland. Dr. Earnshaw's present address is Department of Cell Biology and Anatomy, The Johns Hopkins University School of Medicine, Baltimore, Maryland 21205.

ABSTRACT We have developed procedures for depositing intact mitotic chromosomes and isolated residual scaffolds on electron microscope grids at controlled and reproducible levels of compaction. The chromosomes were isolated using a recently developed aqueous method. Our study has addressed two different aspects of chromosome structure. First, we present a method for improved visualization of radial chromatin loops in undisrupted mitotic chromosomes. Second, we have visualized a nonhistone protein residual scaffold isolated from nuclease-digested chromosomes under conditions of low salt protein extraction. These scaffolds, which have an extremely simple protein composition, are the size of chromosomes, are fibrous in nature, and are found to retain differentiated regions that appear to derive from the kinetochores and the chromatid axis. When our standard preparation conditions were used, the scaffold appearance was found to be very reproducible. If the ionic conditions were varied, however, the scaffold appearance underwent dramatic changes. In the presence of millimolar concentrations of Mg^{++} or high concentrations of NaCl, the fibrous scaffold protein network was observed to undergo a lateral aggregation or assembly into a coarse meshlike structure. The alteration of scaffold structure was apparently reversible. This observation is consistent with a model in which the scaffolding network plays a dynamic role in chromosome condensation at mitosis.

In recent years considerable evidence has been obtained to suggest that the chromatin of both interphase nuclei and metaphase chromosomes is partitioned into closed loop domains containing about 50–100 kilobases of DNA (references below). The existence of chromatin loop domains in interphase nuclei has been suggested by mild digestion of nuclei with nucleases (1, 2) and a number of studies of the supercoiled nature of nuclear DNA after gentle removal of histones (3, 6). The existence of loops in meiotic lampbrush chromosomes has been known for many years (discussed in references 7–9). In these elongated structures the loops are so clearly defined that it has even been possible to identify and map the relative locations of specific loci (8). Loops have also been observed at the periphery of metaphase chromosomes expanded by contact with media of low ionic strength ever since the development of whole-mount microscopy techniques (10–12). It was generally assumed, however, that these loops arose by the untwisting of helical coils (13), since a number of observations suggested that the basic structure of the condensed chromatid might arise from a hierarchy of chromatin coils (see references 14, 15; for a discussion of early models of chromosome architecture, see reference 16).

Examination of chromosomes isolated using a newly developed technique (17) led Stubblefield and Wray to propose that mitotic chromosomes consisted of distinct axial and peripheral chromatin components (18). More recently, when metaphase chromosomes were stripped of histone and examined by surface spreading, loops of DNA were seen surrounding a residual axial structure (19). This suggested a general radial loop model for chromosome architecture (19–21). Support for such a model comes from examination of meiotic prophase chromosomes (22, 23) and from thin-section electron microscopy of swollen metaphase chromosomes (21, 24) and cells (25). In contrast to the radial loop model, helical coil models have also recently attracted attention (26–28). Exposure of chromosomes to a variety of conditions causes them to adopt a helical conformation (14, 15), and this conformation has also been suggested on the basis of microscopy of chromosomes in intact and disrupted nuclei (28). One model proposes that elongated structures sometimes found in chromosome preparations represent a penultimate level of supercoiling which then folds further to give the final compact chromatid structure (26, 27).

THE JOURNAL OF CELL BIOLOGY · VOLUME 96 JANUARY 1983 84-93

What components are responsible for the topological closure of each loop? Evidence presented in previous publications from this laboratory suggests that the loops are held closed at the chromatid axis by nonhistone "scaffolding" proteins (19–21, 29). If the chromosomal DNA was extensively digested with nuclease before removal of histone, it was possible to isolate the residual "scaffold" in stable form (30). Scaffolds isolated in this way preserved the characteristic paired chromatid morphology (30). When examined by SDS gel electrophoresis, they were found to have a complex composition of nonhistone proteins (30).

Lewis and Laemmli have recently reported three new methods for the isolation of chromosomes in aqueous media (32). In the work reported below, we have used one of these methods in which chromosomes are isolated in a polyamine:EDTA buffer similar to that shown to minimize nucleolytic digestion of the DNA during chromosome isolation (33, 34). Polyamine chromosomes isolated as described (32) are virtually free of cytoskeletal contaminants (32). Scaffolds produced from polyamine chromosomes have a greatly simplified protein composition (32). Whereas intact chromosomes are composed of very many proteins, residual scaffolds made from polyamine chromosomes (32) are composed predominantly of two proteins: SC1 (M_r, 170,000 daltons) and SC2 (M_r, 135,000 daltons) (32). These two proteins comprise at least 40% of the overall protein mass of the scaffolds.

Residual scaffolds are interesting subjects for structural analysis both because they have a limited and specific protein composition and because they retain the ability to hold metaphase DNA in a partly compact fast-sedimenting form (32). Interestingly, the metaphase scaffolding is a metalloprotein structure containing Cu^{++} (or possibly Ca^{++}) which stabilizes this structure against dissociation by histone extraction buffers (32). Chelating of the metal leads to dissociation of the scaffolding and to a complete unfolding of the DNA (32).

We have developed procedures for depositing intact chromosomes and isolated residual scaffolds on electron microscope grids at controlled and reproducible levels of compaction. We have achieved an improved visualization of radial chromatin loops in intact chromosomes and have also been able to observe what appear to be axial structures in spread preparations of intact chromosomes. We have found that isolated scaffolds can exhibit an extreme variability of appearance, arising at least in part from the fact that they contract and expand in an apparently reversible way in response to alterations in ionic strength. Finally, we show that under carefully controlled conditions isolated scaffolds exhibit a reproducible appearance with well defined substructure. Notably, residual scaffolds in which histone is undetectable in SDS gels appear to retain differentiation of the kinetochore region.

MATERIALS AND METHODS

Chromosome Isolation: Chromosomes were purified from colcemid-arrested HeLa cells by the polyamine method of Lewis and Laemmli (32) with the following modification. After the Percoll gradient, the chromosome band was mixed with 50 ml of buffer containing 5 mM Tris:HCl pH 7.4, 0.25 mM spermidine, 2 mM K-EDTA pH 7.4, 2 mM KCl; and this solution was homogenized gently (four strokes in a Wheaton homogenizer: Wheaton Scientific, Millville, NJ). The solution was diluted with an equal volume of buffer and centrifuged for 30 min at 1,100 *g* at 4°C (Clay Adams Dynac Centrifuge, Parsippany, NJ). The pellets were gently resuspended in 1–2 ml of 5 mM Tris:HCl pH 7.4, 0.25 mM spermidine, 2 mM KCl (buffer 4).

Scaffold Isolation: In a typical experiment, 0.3 ml of chromosomes (350 μg protein/ml [35]) was mixed with 0.6 ml buffer 4; $CaCl_2$ was added to 1 mM; 15 μg of micrococcal nuclease (Millipore Corp., Freehold, NJ) and 9 μl of Trasylol (Aprotinin-Mowbay Chemical Co., FBA Pharmaceuticals, New York, NY) were added and the mixture was incubated at 4°C. In some experiments, 6 μg of RNaseA (Millipore Corp.: heated for 10 min at 100°C) was also added. After 30 min, $CuSO_4$ was added to 0.3 mM under an atmosphere of N_2. After 10 min at 4°C, Na-EDTA (pH 9) was added to 2 mM.

0.9 ml of the above was mixed with 1.8 ml of 1 mM triethanolamine:HCl pH 8.5, 0.2 mM Na-EDTA pH 9 (TEE buffer) and to this was added 2.7 ml of 2x lysis mixture containing 20 mM Tris pH 9, 20 mM Na-EDTA pH 9, 0.2% Ammonyx Lo, 0.4 mg/ml dextran sulfate, and 0.04 mg/ml heparin. The polyanion concentration was 10-fold lower than that used by Lewis and Laemmli (32). In certain experiments the polyanions were replaced by 4 M NaCl, with the other components being the same. After 20 min at 4°C, 50 μl was sedimented onto a carbon-coated electron microscope grid through a cushion of 1× lysis mixture plus 0.1 M sucrose. The rest of the solution was processed for SDS PAGE as described previously (32).

Scaffolds with identical biochemical properties may be produced by both high ionic strength (2 M NaCl) and low ionic strength (dextran sulfate:heparin) histone extraction procedures (29, 32). That the two procedures work by different mechanisms is suggested by the observation that the presence of NaCl in concentrations as low as 12 mM causes a significant decrease in the efficiency of protein extraction by the polyanion lysis mixture (data not shown). The conductivity of the dextran sulfate:heparin lysis mixture used is comparable to that of a 20 mM solution of NaCl (and is mostly due to the 10 mM EDTA present in the mixture—data not shown). At similar ionic strength, chromosomes are highly expanded (Fig. 1*a*). We would expect that the dextran sulfate:heparin lysis mixture would cause a minimum of protein precipitation both because of its low ionic strength and because of the general solubilizing effect which polyanions have on chromatin (36, 37).

The observation that residual scaffolds may be produced in hypotonic solutions was presented in the first paper of this series (19). Those results, together with the finding that NaCl actually antagonizes the hypotonic extraction procedure, suggest that the hypothesis advanced by some workers that residual scaffolds are formed by nonhistone protein aggregation in the presence of high salt (38, 39) is unlikely.

For the scaffold shrinkage:swelling experiment of Fig. 8, after 10-min incubation with lysis mix, 200 μl of solution were withdrawn into another tube and 40 μl of 10× RSB (100 mM Tris:HCl pH 7.4, 100 mM NaCl, 50 mM $MgCl_2$) were added. After 5 min, 120 μl of this solution were added to 13 μl of 100 mM Na-EDTA pH 9. After another 5 min at 4°C, the scaffolds were centrifuged through either 1× lysis mix plus 0.1 M sucrose or 1× RSB plus 0.1 M sucrose, dextran sulfate, and heparin (as in the lysis mix).

Determination of Scaffold Composition: Chromosome purification and scaffold isolation were done as described above, except that chromosomes were labeled in vivo with [^{35}S]methionine, [^{3}H]uridine, or ^{3}H-thymidine. The three cultures were grown and labeled in parallel. The specific activity of [^{35}S]methionine was calculated following determination of protein by the Folin method (35) modified to include 1% SDS (40). The specific activity of [^{3}H]uridine was calculated by taking an aliquot of material from the top of the sucrose gradient during chromosome isolation (32), centrifuging it at 60,000 *g* for 1 h, and determining the A_{260} of the supernatant in the presence of 0.1 N NaOH. This material was at least 84% single stranded, as deduced from the A_{260} in the presence and absence of 0.1 N NaOH (41). The specific activity of [^{3}H]thymidine was estimated by assuming a 2:1 ratio of protein to DNA in purified chromosomes (Lewis, unpublished). For estimation of relative composition, equal volumes of chromosomes were used to prepare scaffolds (defined as material which sedimented to the bottom of the centrifuge tube after centrifugation at 5,000 *g* for 30 min) in paralle, and amounts of protein, RNA, and DNA were determined from the specific activity of label. The three samples were normalized to equal chromosome input based on protein concentration in the presence of 1% SDS (40). The values presented in the text are the average from three such experiments.

Electron Microscopy: In the course of this study it was determined that exposure of hydrated chromosomes or scaffolds to a number of agents (among them ethanolic phosphotungstic acid and 2% aqueous uranyl acetate) would cause the structures to undergo radical contraction, even if they were adsorbed to a carbon film and fixed with 2% glutaraldehyde. To "lock" expanded structures in an expanded conformation before exposure to stain, it was necessary to dry them thoroughly. We will refer to this procedure involving drying of the grids before staining as procedure A.

In certain cases it was desirable to allow contact with stain to cause the structure to shrink. In this case the drying step before staining was omitted, all other steps being identical. We will refer to this approach as procedure B.

After centrifugation of the scaffolds onto the carbon-coated electron microscope grid (1,400 *g* for 20 min at 4°C), the supernatant was removed by aspiration and replaced with 0.4% Photoflo (Kodak) as suggested by Labhardt and Koller (42). For Figs. 1, 6, and 7, the grids were then processed by procedure A. That is,

the grids were rinsed in 0.4% Photoflo and fixed in TEE buffer plus 1% glutaraldehyde (BDH general purpose solution) for 1–2 h at 4°C. The grids were then blotted dry and allowed to stand until thoroughly dry. Each grid was then dipped into 1% phosphotungstic acid (PTA) in 71% ethanol for 15 s, rinsed in 95% ethanol for 15 s, rinsed in 0.4% Photoflo for 5 s, blotted dry, and rotary shadowed with platinum:palladium. For Figs. 2 and 3, procedure B was used. The carbon grids used for Figs. 2 and 3 were pretreated with Alcian blue (Serva, Heidelberg—see reference 42). The grid for Fig. 5 was processed by procedure A, except that the PTA stain was replaced by 2% uranyl acetate, 1% dimethyl sulfoxide and subsequent rinsing and rotary shadowing were omitted. For Fig. 5 the carbon film was rendered hydrophilic by glow discharging.

All electron microscopy was performed with a Philips EM-300 at 80 kV.

RESULTS

Electron Microscopy of Purified Chromosomes

EXPANDED AND CONDENSED FORMS: If purified chromosomes are placed in a solution of very low ionic strength they expand greatly (43). When such expanded chromosomes are sedimented onto a carbon-coated electron microscope grid, they lose the characteristic paired chromatid morphology, resembling instead a puddle of chromatin (Fig. 1 *a*). This puddle retains certain aspects of chromosome structure. In favorable samples, the axis of each chromatid remains distinguishable, implying that this region may differ structurally from the bulk of the chromatin, which is dispersed with a uniform density. Additionally, the centromere region retains its differentiation, with apparent kinetochores visible as twin dark spots. The axial structure with attached kinetochores may correspond to a nonhistone scaffold which might organize the chromatin and maintain chromosome integrity under these highly dispersive conditions.

The swelling process is dynamic, and expanded chromosomes adsorbed to carbon films respond to changes in ionic milieu. Fig. 1 *c* shows chromosomes prepared in parallel with that in Fig. 1 *a* (i.e. deposited on the grid in swollen form) but exposed on the grid to a solution containing 5 mM Mg^{++} (RSB buffer). The bulk of the chromatin has contracted back onto the chromatid axis in an apparently ordered way. Since much of the chromatin was adsorbed to the grid, the contraction is not completely uniform. In addition to contracting towards the chromosome axis, some chromatin is also seen to aggregate laterally, forming cables which are attached to the carbon film at their outer tips.

For comparison, Fig. 1 *b* shows a compact chromosome which was sedimented onto the electron microscope grid through a solution containing divalent cation (RSB buffer). Little substructural detail is visible.

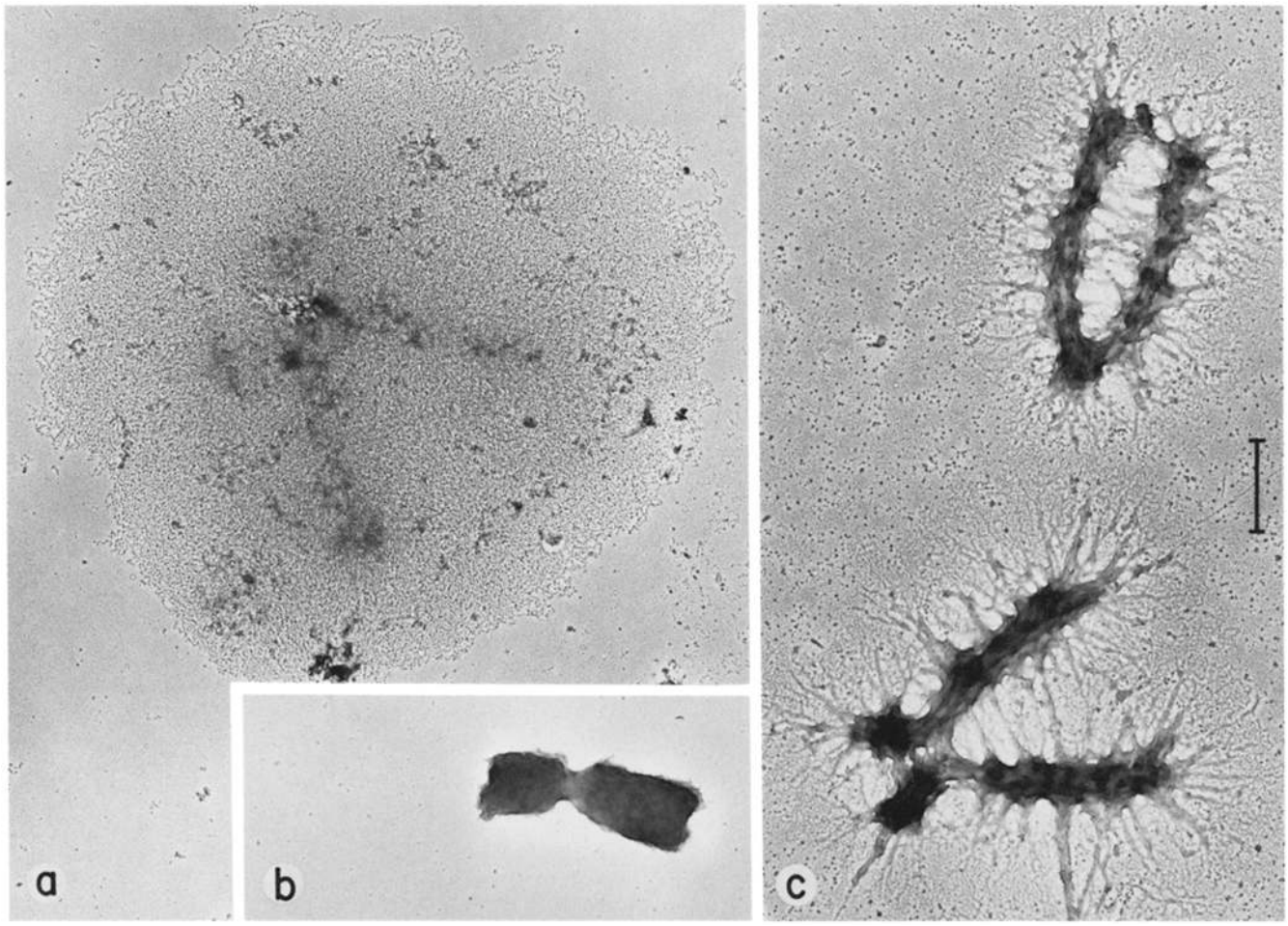

FIGURE 1 Swelling and shrinking of chromosomes. (*a*) Chromosome swollen by exposure to buffer of low ionic strength containing 0.2 mM EDTA, and subsequently centrifuged onto an electron microscope grid. Note the dark-staining kinetochores and dense material remaining on the chromatid axes. (*b*) Condensed chromosome. Chromosomes from the swollen preparation used in *a* were exposed to 5 mM Mg^{++} before sedimentation onto the microscope grid. (*c*) Chromosome shrinkage on the surface of the grid. A grid prepared in parallel with that in *a* was briefly exposed to 5 mM Mg^{++} before fixation. Bar, 1 μm.

ORGANIZATION OF CHROMATIN IN METAPHASE CHROMOSOMES: The puddle of chromatin which surrounds the axial elements in Fig. 1 *a* is so evenly dispersed that no detail of the path of individual fibers is visible. We noticed that this expanded morphology was observed if the grids were dried before staining. This seems to "freeze" the chromosome in the expanded state. If the drying step was omitted, chromosomes which were prepared in parallel presented a different appearance in the electron microscope (Fig. 2). We interpret this result to show that exposure of hydrated expanded chromosomes to stain causes the bulk of the chromatin to contract back onto the chromatid axes, while chromatin adsorbed to the film remains expanded.

The latter chromatin is seen to form loops which emanate from points along the length of the chromatid axis (Fig. 2 *a*), while the bulk of the material is seen to condense into a dense mass along the axis covering the base of the loops. A higher magnification view (Fig. 2 *b*) clearly shows the expected nucleosomal organization of the loop chromatin. On the basis of the maximum loop radius we observe, we estimate that the average chromatin loop in our spreads is about 4.6 ± 1.6 μm long. Since our spreads were made under conditions where we would not expect higher-order packing of nucleosomes (44), we estimate that this corresponds to 83 ± 29 kb per loop (assuming a linear packing ratio for the nucleosome of 6.2; see reference 45).

In all purified chromosome preparations a variable number of dense fiberlike structures is observed. These are normally rare in our preparations, but their frequency may be increased by intentionally exposing the chromosomes to shear. The structures resemble "unit-fibers" described previously by other workers (26, 27). In a preparation which had been exposed to shear by repeated pipetting through an uncut micropipette tip, we were able to observe normal chromosomes, fibers, and intermediate structures. Fig. 3 shows such an intermediate. Evidence from structures observed at different stages in the chromosome-to-fiber transformation (not shown) suggests strongly that these images do not arise from chance juxtaposition of separate chromosome and fiber structures. The dense fiber does not give rise to radial chromatin loops, while attached regions of untransformed chromatin do. In regions where the fiber is less condensed, limited numbers of small loops may be seen, confirming that the fiber is composed of chromatin. These data suggest that the packing of chromatin in dense fibers and in normal chromosomes is different. We suggest that the fibers arise from damage to chromosomes during handling in vitro and not from a simple unfolding of the chromosome higher-order structure as had been proposed (26, 27).

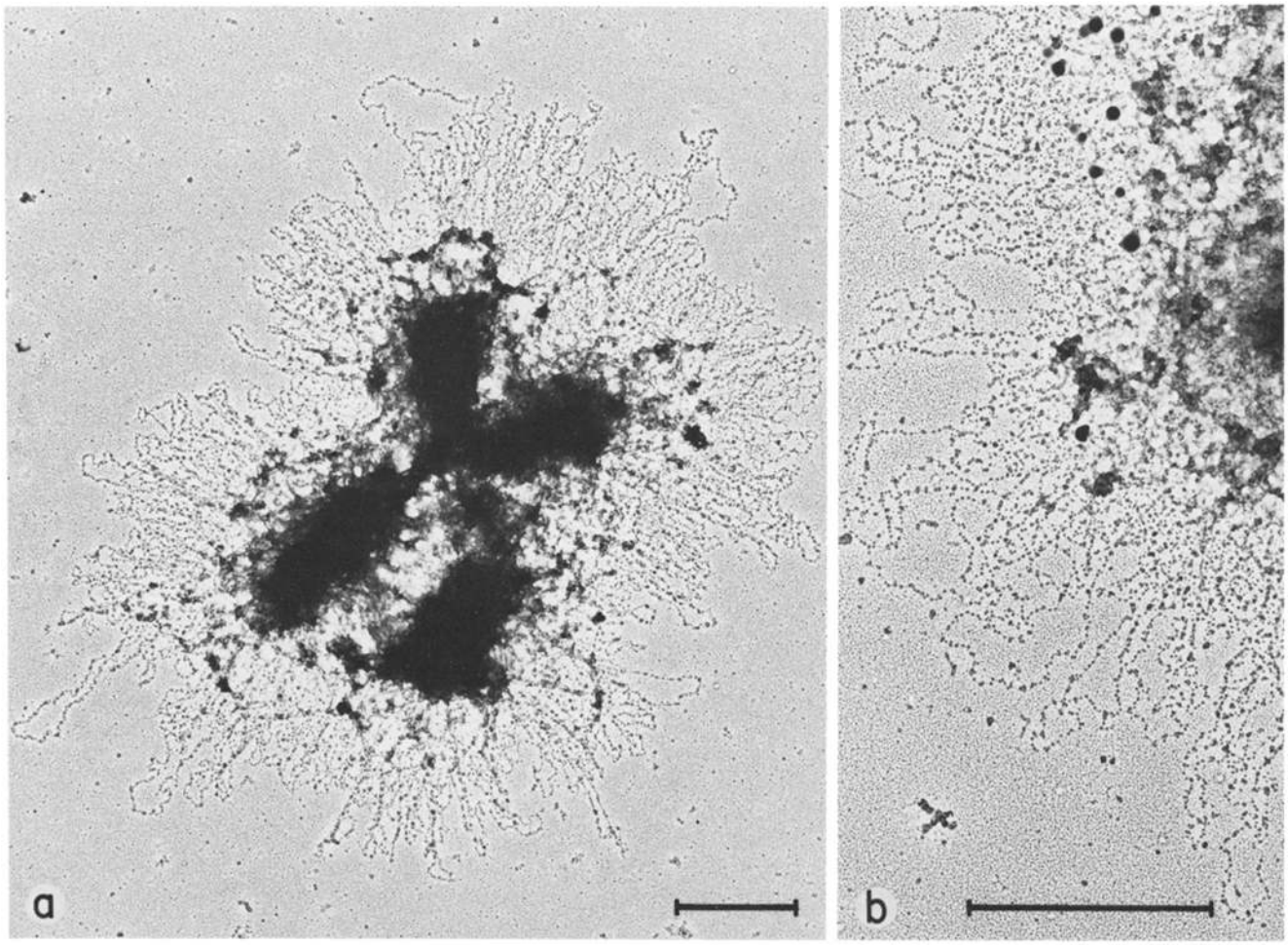

FIGURE 2 Radial loops of chromatin in undisrupted chromosomes. (*a*) Whole chromosome showing radial loops emanating from points all along the chromatid arms. (*b*) Higher magnification view showing the nucleosomal arrangement of the chromatin in the loops. When deposited on the carbon film, the chromosomes were swollen like that in Fig. 1 *a*. All chromatin not in contact with the film was then caused to contract by exposure to ethanolic PTA while the chromosome was still in hydrated form.

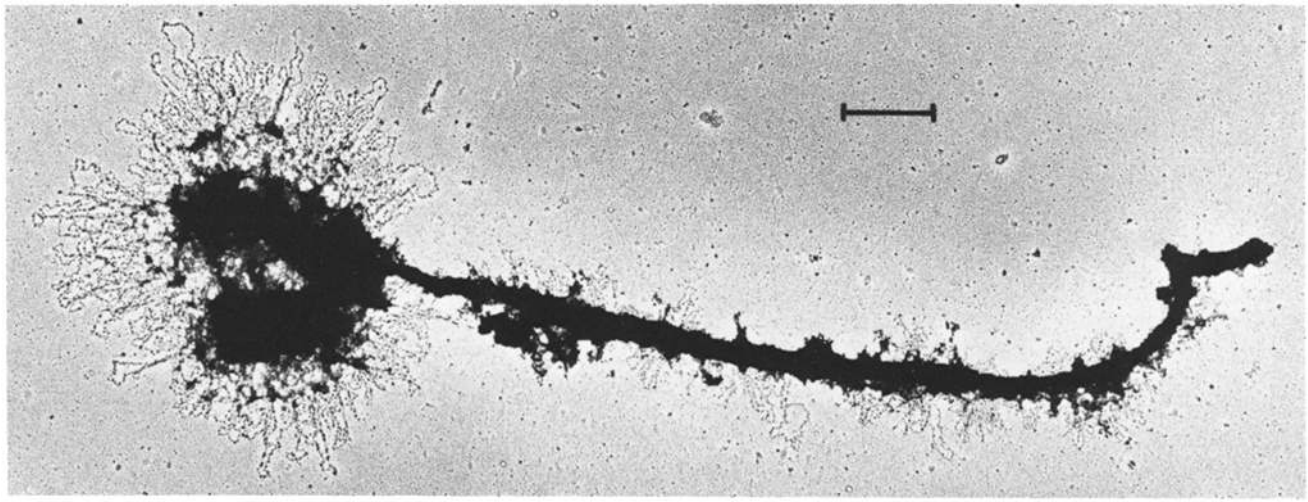

FIGURE 3 Absence of radial loops on dense fibers derived from chromosomes. A chromosome preparation was forcibly pipetted through an uncut pipette tip, resulting in production of dense fibers. The chromosomes were then treated as in Fig. 2. Note the presence of radial loops on the chromosomes, and their absence on the fibers. In this figure small loops are seen where the fiber is less dense, but many examples were found where no hint of loops could be seen.

The above results support a loop model for metaphase chromosome architecture (19–21). An inherent part of such a model is the requirement for structural components which are attached to the base of each loop, causing it to be topologically closed. These components have been termed "scaffolding proteins" (29). Evidence from this laboratory suggests that the scaffolding proteins are not histones but rather an extremely limited subset of the chromosomal nonhistone proteins (32). We present, below, results of a study of the structure of isolated chromosome scaffolds.

The Structure of Residual Scaffolds

BIOCHEMICAL CHARACTERIZATION: For this work we have slightly altered the procedures of Lewis and Laemmli (32) for production of residual scaffolds from nuclease-digested chromosomes to optimize the structural preservation of the scaffolds. These modifications do not appear to affect the biochemical properties of the scaffolds as originally described (32). We found that residual scaffolds retaining 4–7% of the total protein consisted predominantly of two high molecular weight proteins (Sc1: M_r, 170,000; Sc2: M_r, 135,000) previously described by Lewis and Laemmli (32). Fig. 4 shows an SDS polyacrylamide gel of scaffolds prepared from ^{35}S-methionine-labeled chromosomes. From the gel it may be seen that histones are not detectable in scaffolds and that, relative to the two high molecular weight proteins Sc1 and Sc2, all other protein components are present in greatly reduced amounts. In the experiment shown, when the autoradiograph was scanned and bands were cut out and weighed, it was determined that Sc1 and Sc2 comprised about 40% of the total ^{35}S-methionine-labeled protein. Therefore, while Sc1 and Sc2 appear to be the most abundant components of scaffolds, it is likely that many minor protein species also contribute to structural detail observed in the electron microscope.

All preparations used for electron microscopy were monitored by SDS PAGE. While we have found some variation in the amount of nonhistone protein remaining in scaffolds, possibly due to daily variation in the condition of the cells, we have never detected any histone in our gels, even when amounts loaded were such that the histone in control tracks was heavily

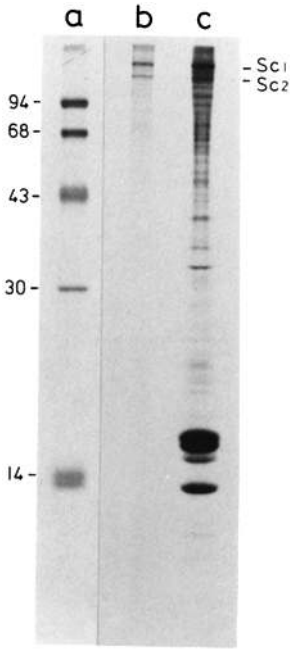

FIGURE 4 SDS polyacrylamide gel of residual scaffolds containing 4–7% of the [^{35}S]methionine-labeled chromosomal protein. Scaffolds were produced as described in Materials and Methods and subjected to electrophoresis as described previously (32). (Track *a*) Marker proteins (phosphorylase b— M_r = 94,000; bovine serum albumin— M_r = 68,000; ovalbumin— M_r = 43,000; carboic anhydrase— M_r = 30,000, cytochrome *c*— M_r = 14,000). (Track *b*) Residual scaffolds produced by exposure of nuclease digested chromosomes to dextran sulphate:heparin lysis mix. (Track *c*) Nuclease-digested chromosomes before polyanion extraction. Equal amounts of chromosomes were used for tracks *B* and *C*. The separating gel was 13% acrylamide.

overloaded. We cannot explain why procedures for production of chromosome "scaffolds" published by other labs have failed to achieve complete extraction of the histones (38, 46). This may be due to the "toughening" affect of calcium on nuclear structures (31, 32), or it could be due to the fact that in our protocol particular care was taken to prevent reassociation of histone with the residual scaffolds during specimen preparation for electron microscopy and gel electrophoresis, as described in Materials and Methods.

SCAFFOLD APPEARANCE IN THE ELECTRON MICROSCOPE: Fig. 5 shows a well-preserved scaffold observed in positive contrast with uranyl acetate stain. A survey micrograph at lower magnification is presented in Fig. 6*a*. A number of conclusions may be drawn from these micrographs.

(*a*) Scaffolds may be isolated from chromosomes prepared in aqueous solutions. Therefore, exposure of chromosomes to hexylene glycol (17, 29) is not required for scaffold stability.

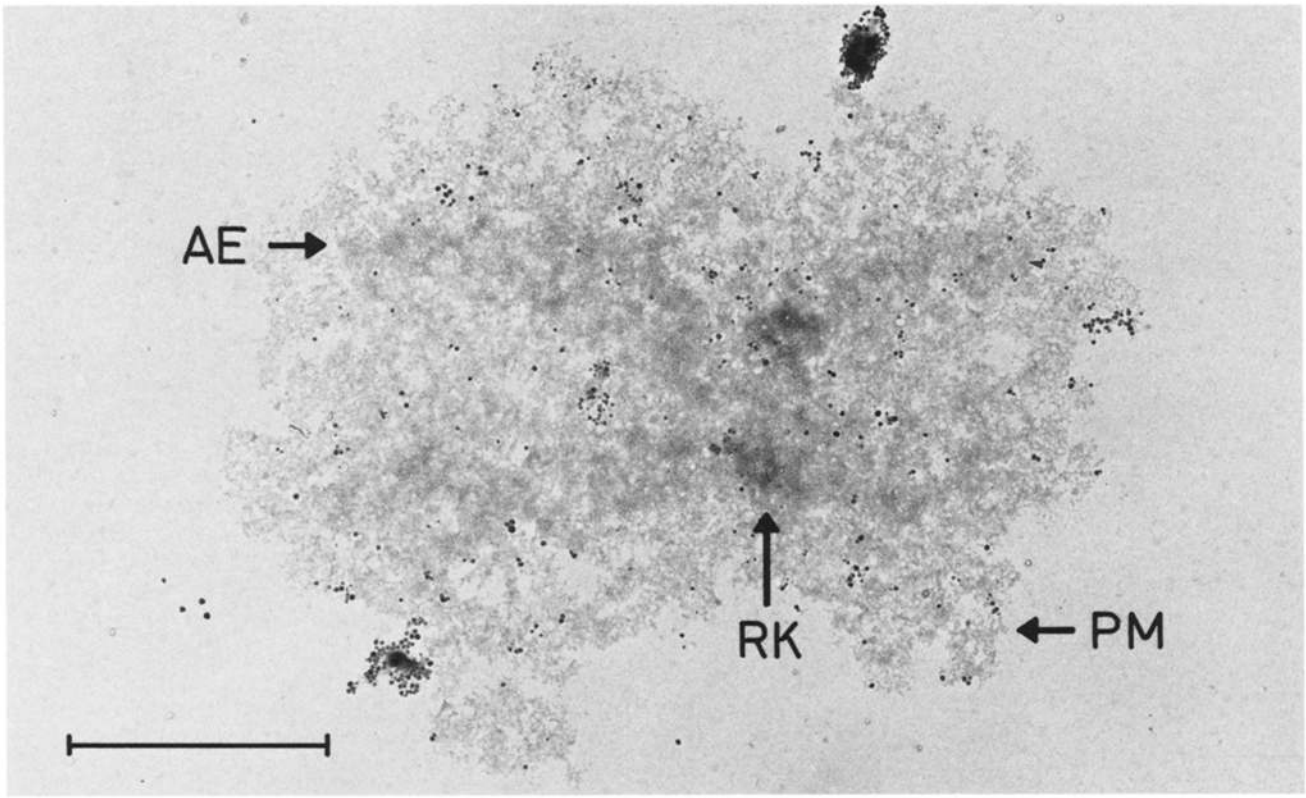

FIGURE 5 Residual chromosome scaffold contrasted in uranyl acetate positive stain. The scaffold was produced by polyanion treatment of nuclease-digested chromosomes. Three features of scaffold morphology are seen: apparent residual kinetochores (*RK*), axial elements (*AE*), which follow the path of the chromatid arms, and peripheral material (*PM*). The dark round objects of ~300 Å diameter are Percoll. The grid was dried thoroughly before staining.

(*b*) Scaffolds retain the dual nature of paired mitotic chromatids (30). Therefore the sister chromatids are held together either by protein or by nucleic acid which is protected from digestion by micrococcal nuclease and RNaseA. In many scaffolds, the distinction between sister chromatids is lost due to fusion of the two arms, though images may be obtained where the arms remain separate. (*c*) Well-preserved scaffolds display a pattern interpreted in terms of three distinct structural features: apparent residual kinetochores (RK), axial elements (AE), and peripheral material (PM). These are indicated in Fig. 5. In general, the ease of observation of apparent residual kinetochores is linked with the overall degree of scaffold preservation. (*d*) Even though scaffolds retain only 5–10% of the total chromosome mass (including nucleic acid; see below), they were found to be large structures, roughly 60–80% of the length of intact chromosomes. This suggests that the scaffold is likely to be derived from a protein network which was continuous throughout the chromosome. (*e*) As described in Materials and Methods, during scaffold production purified chromosomes were digested with nuclease before removal of histone. The scaffolds obtained were indistinguishable regardless of whether RNaseA was or was not present in addition to micrococcal nuclease during this digestion. We conclude that the structural features we observe (including apparent residual kinetochores) are not due to the presence of RNA, at least in digestible form.

Since the scaffolds observed in our experiments were large structures retaining many structural features of intact chromosomes, we wished to determine to what extent the structural detail could be due to residual nucleic acid. Under our conditions, the mass of residual scaffolds was 95 ± 3.5% protein, 2.0 ± 1.1% DNA, and 2.7 ± 3.0% RNA. The amount of residual nucleic acid can be lowered further under different digestion conditions (30), but it was low enough in these experiments for us to conclude that the bulk of the structural detail observed in the electron microscope is probably due to protein.

Lewis and Laemmli (32) have shown that treatment of scaffolds with β-mercaptoethanol or metal chelators (orthophenanthroline or neocuproine) causes the structures to fall apart. When a scaffold preparation was treated with 50 mM β-mercaptoethanol and then sedimented onto an electron microscope grid as described in Materials and Methods (with addition of β-mercaptoethanol to the sucrose cushion), no recognizable structures were observed (data not shown).

VARIATION IN SCAFFOLD APPEARANCE: Even though residual scaffolds obtained after histone removal by treatment of nuclease-digested chromosomes with either 2 M NaCl or dextran sulfate:heparin lysis mixtures have identical biochemical properties, they appear quite different when examined in the electron microscope. Fig. 6 *a* shows a particularly favorable field of scaffolds prepared by dextran sulfate:heparin extraction. Residual kinetochores, axial elements, and peripheral material may be seen in most of the scaffolds. The general morphological preservation of scaffolds produced by 2 M NaCl was inferior (Fig. 6 *b*). In general, these structures appeared extremely condensed and did not show the substructural elements seen in more expanded scaffolds. Occasionally, however, it was possible to find examples where what were apparently residual kinetochores could be observed (Fig. 6 *b*).

In obtaining negative stain images of scaffolds, we again observed the presence of contracted and expanded forms.

Expanded scaffolds could be "frozen" in the expanded conformation by drying before staining. The scaffold in Fig. 5 comes from a positively stained area of such a grid. Where expanded scaffolds were negatively stained, it was difficult to resolve details of the finely dispersed protein network (data not shown). If scaffolds prepared by dextran sulfate:heparin extraction were stained with uranyl acetate while hydrated, they became much more compact. The scaffold material was found to condense into cables which interweave to form a meshlike network.

REVERSIBLE ALTERATION OF SCAFFOLD MORPHOLOGY: The results presented above show that isolated residual scaffolds may exist in two conformations: an extremely diffuse fiber network (expanded form) or a condensed network. The experiment presented in Fig. 7 shows that the condensation process is apparently reversible. Conditions were chosen which would cause intact chromosomes to condense and then to reexpand (Fig. 1).

The scaffolds of Fig. 7 *a* (prepared by dextran sulfate:heparin extraction) are highly expanded. Substructural detail is difficult to visualize, though diffuse residual kinetochores and axial elements are detectable in some structures. When these expanded scaffolds were exposed to 5 mM Mg^{++} (in this case added as RSB buffer), they were found to contact into compact structures resembling scaffolds produced by histone removal with 2 M NaCl (Fig. 7 *b*; compare with Fig. 6 *b*). This alteration in scaffold morphology was apparently reversible, since if EDTA was added to 10 mM the scaffolds expanded once again (Fig. 7 *c*). In the reexpanded scaffolds the characteristic scaffold substructures are clearly seen even though these were difficult to detect initially. This is because the reexpanded scaffolds remained slightly more compact than the starting material, and it emphasizes that observation of substructural detail in isolated scaffolds is dependent on the overall level of scaffold compaction.

In our experiments, dextran sulfate:heparin-prepared scaffolds which had been exposed to Mg^{++} were smaller than expanded structures (by ~40% in length and 25% in width). This was consistent with earlier results which showed that scaffolds in the presence of 2 M NaCl were ~50% shorter than scaffolds in 0.1 M NaCl (14). Even more than the size change, the most striking difference between expanded and compacted scaffolds lay in the extent of lateral association of the scaffold fibers. The compacted structures of Fig. 7 *b* appear substantially more "coarse" than those of Fig. 7 *a*. This coarse fiber mor-

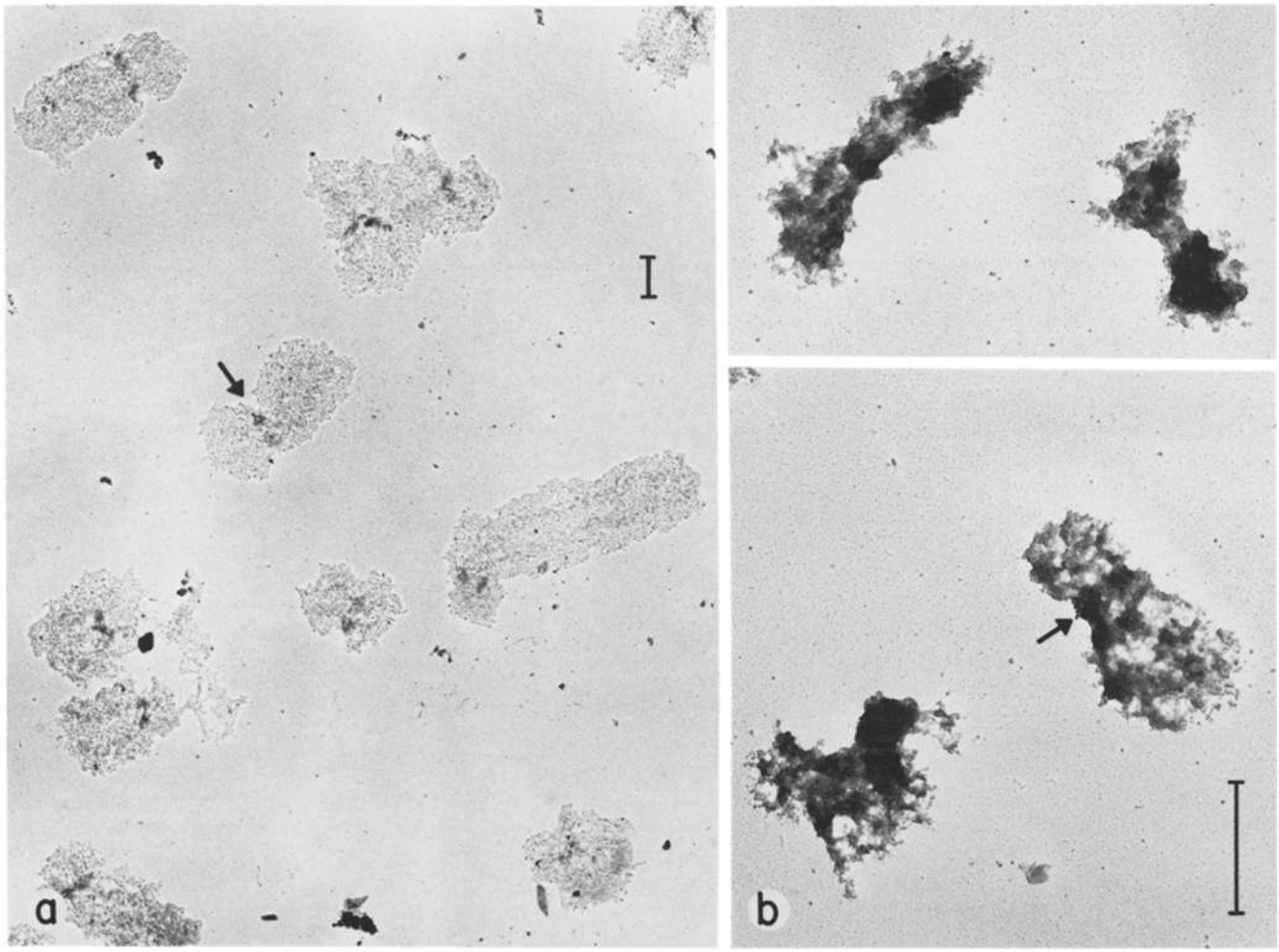

FIGURE 6 Effect of lysis procedure on scaffold morphology. (*a*) Scaffolds produced at low ionic strength by histone extraction with dextran sulphate:heparin. Observation of residual kinetochores (arrow), axial elements, and peripheral material is possible in most of the structures. (*b*) Scaffolds produced in parallel by removal of histone from nuclease-digested chromosomes in the presence of 2 M NaCl. These contracted structures exhibit poor structural preservation but occasionally show what are apparently residual kinetochores (arrow).

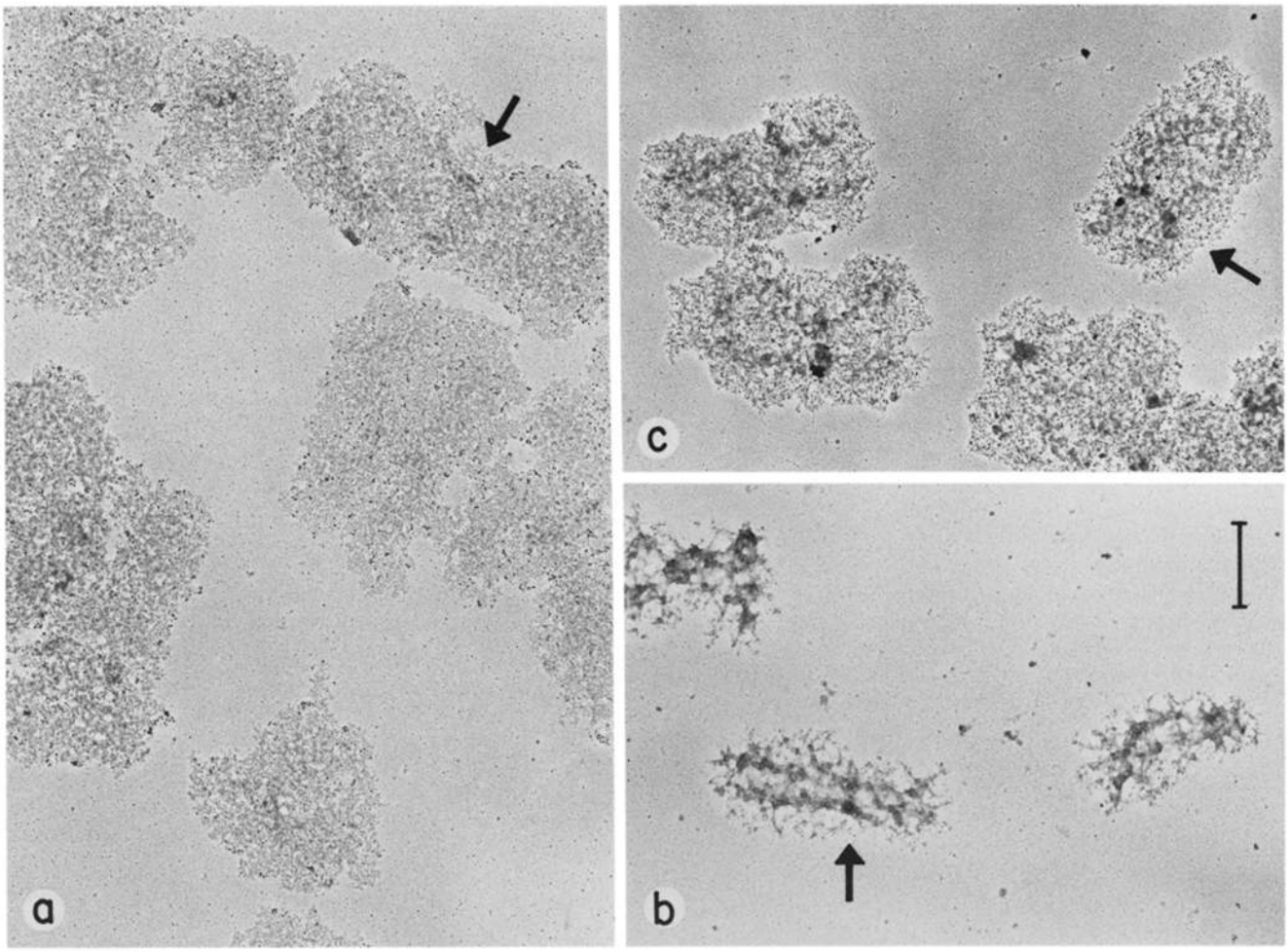

FIGURE 7 Reversible scaffold swelling and contraction. (*a*) An expanded scaffold preparation. These scaffolds are somewhat more expanded than those in Fig. 6 *a*, and consequently the residual kinetochores (arrow) are more difficult to see. (*b*) An aliquot from the scaffolds in *a* which was exposed to 5 mM Mg^{++} in solution as described in Materials and Methods. These scaffolds have adopted a coarse fibrous morphology. (*c*) An aliquot from *b* to which 10 mM EDTA was added to chelate the Mg^{++}. Note that the apparent residual kinetochores, axial elements, and peripheral material remain visible throughout the entire process.

phology was also observed on shadowed preparations where Mg^{++} alone was added to the lysis mix rather than RSB buffer (data not shown).

DISCUSSION

Observation of Chromatin Loops

Early reports on whole-mount techniques (10, 47) showed that chromatin loops could be observed at the periphery of metaphase chromosomes (12, 13, 48). In general, these studies showed only the distal tips of the loops, with an occasional loop being more extended. We have extended these observations and developed a reproducible method for visualization of an array of loops which projects evenly from all parts of the chromosome axis. Our photographs resemble images of meiotic prophase chromosomes (22, 23), although in the latter, which are more extended than metaphase chromosomes, the loops could be observed directly. These results, together with results of thin-section electron microscopy (21, 24, 25), support a loop model of metaphase chromosome architecture.

We have also shown that dense fiberlike structures derived from metaphase chromosomes (26, 27) do not give rise to radial loops under our spreading conditions. The fibers expand upon hypotonic treatment (not shown), so the failure to give rise to loops is not due to an inability of the chromatin to disperse. Since intact chromosomes give rise to loops while dense fiber structures do not, we suggest that the fibers do not arise from a simple unfolding of the chromosome as was previously suggested (26, 27). We propose that the fibers arise from an alteration of the normal structure, resulting from exposure to excessive shear during manipulation in vitro.

An alternative model for metaphase chromosome architecture suggests that chromosomes are constructed from a hierarchy of helices and superhelices (13–15, 26–28). Our data, and those data cited above, suggest that the chromatin is restrained in radial loops, possibly by interaction with axial scaffolding proteins. It is possible that such an axial scaffolding network might itself assemble with helical symmetry, in which case the chromosome could appear to possess helical symmetry under certain circumstances (14, 15, 28). In this case, the chromatid could be viewed as a helix with each subunit consisting of a chromatin loop attached to a unit of axial nonhistone scaffold. A second possibility, suggested by Bahr (13), is that the loops arise by an untwisting of supercoiled regions.

Do Intact Chromosomes Contain a Nonhistone Scaffold

The existence of chromatin loops in chromosomes suggests that these loops may be topologically closed due to binding of

proteins which bridge the base of each loop. We refer to these hypothetical proteins as "scaffolding proteins." In a model proposed earlier by this laboratory, lateral interactions among these proteins were postulated to be responsible for maintaining the condensed state of the chromosome (19, 20, 29).

In expanded chromosomes it is sometimes possible to observe structural elements which follow the path of the chromatid axes (Fig. 1 *a*). We believe this to be the first direct visualization of the scaffold in an intact chromosome.

An additional suggestion that chromatin in metaphase chromosomes might be attached to structural components along the chromatid axis comes from the experiments of Figs. 1 and 2. When chromosomes are exposed to ionic conditions where chromatin is highly soluble, they expand greatly (see also the careful study by Cole [43]) and lose the defined double chromatid shape. When these expanded "puddles" of chromatin are exposed to conditions where chromatin is condensed, expanded chromatin contracts back onto the chromatid axes in an apparently organized manner.

Additional evidence for the existence of axial nonhistone scaffold elements in metaphase chromosomes comes from silver staining experiments. Silver, which contrasts the "scaffold" elements of meiotic synaptonemal complexes (49–51), may under certain conditions also be shown to stain an axial "core" in mitotic chromosomes (52, 53). In recent experiments we have used a modification of the Ag-As silver staining procedure (54) to show that isolated residual scaffolds and intact chromosomes are stained specifically under identical conditions (Earnshaw and Laemmli, manuscript submitted for publication). This suggests that the "core" structure seen in intact chromosomes corresponds to the residual scaffolds presented in this study.

Other workers have failed to directly observe scaffold structures in intact chromosomes (38, 39). This could be due, in part, to a misapprehension as to the amount of protein in the scaffold and its distribution in the chromosome. The scaffold retains about 3–4% of total chromosomal protein (32) yet remains nearly the size of an intact chromosome. Examination of Figs. 5–7 shows that the isolated scaffold is a diffuse structure which is likely to extend throughout the entire chromosome and not just along the axis. Such a diffuse structure would be extremely difficult to detect in the presence of a 40-fold weight excess of chromatin unless specific stains (such as silver) were used. In fact, it is even difficult to detect isolated expanded scaffolds against a background of light negative stain (not shown).

Published evidence suggests that the isolated scaffolds we observe do not arise from nonspecific precipitation of chromosomal proteins, since identical structures are obtained after histone removal by differing mechanisms at either high or low ionic strength (30, 32; see Materials and Methods). Together, the simple and repeatable protein composition of scaffolds (32), the observation that the scaffold requires specific metalloprotein interactions for stability (32) and the electron microscope studies presented in this report support the hypothesis that the isolated scaffold is a defined structure, not a nonspecific aggregate.

Electron Microscopy of Isolated Residual Scaffolds

Since the study of scaffolds *in situ* is not yet possible, we have instead performed a structural analysis of isolated residual scaffolds. Electron microscopy of the residual scaffold is difficult, principally because the large size of the structures makes them fragile and easily subject to distortion during specimen preparation. Nonetheless, a number of conclusions may be drawn about scaffold structure from our micrographs.

(*a*) Residual scaffolds appear to be derived from a fiber network which extends throughout the entire chromosome. (*b*) Isolated scaffolds retain the paired sister chromatid morphology, though the separation between the chromatids is generally indistinct. (*c*) A differentiated region, apparently derived from the kinetochore, remains visible. We do not know what fraction of kinetochore components is retained or whether the structure remains capable of binding microtubules. We are currently attempting to identify the kinetochore components which remain in scaffolds. (*d*) The central axis of each chromatid remains visible in many scaffolds. Apparently, the scaffolds contain material which was located centrally in the chromatid arms as well as material which was peripheral. The central material may contain the proteins which act as fasteners for the chromatin loop domains. The peripheral material may also have been associated with the chromatin loops but in regions distal to the central axis. (*e*) In the presence of millimolar amounts of Mg^{++}, scaffolds undergo a morphological change. This change appears to be primarily a coalescence of fine fibers into coarse cables (see Fig. 7). It is apparently reversible. Since intact chromosomes undergo a swelling and shrinking response under similar ionic conditions, it seems reasonable to postulate that the chromosome response might in part be due to alterations of the scaffold structure. Note, however, that the ionic conditions used would have a similar effect on chromatin alone, so for chromosomes it is not possible to separate the effects due to chromatin from those due to scaffold.

Mitotic Chromosome Condensation

It seems likely that radial loops in metaphase chromosomes (70 kb: see reference 19; 83 + 28 kb: this study) correspond to chromatin domains detected in interphase nuclei by a number of techniques: nuclease digestion (1, 2), sedimentation (3–5), and fluorescence microscopy (6). The interphase domain sizes suggested from these results are 75 kb (1), 80 kb (2), 85 kb (3), 220 kb (4), 136 kb (5), and 84–96 kb (6).

Because similar chromatin domain sizes are found for both mitotic chromosomes and interphase nuclei, it is possible that, at the domain level, the ordering of chromatin is similar throughout the cell cycle despite the enormous increase in degree of chromatin condensation which occurs during mitosis. The problem of chromosome condensation at mitosis may be regarded as one of changing the organization of the domains from an open network dispersed throughout the entire nucleus into a number of discrete entities suitable for partitioning between daughter cells (i.e. condensed metaphase chromosomes). A similar model has also been suggested from the analysis of interphase HeLa nuclear scaffolds (31).

During mitotic prophase the scaffold proteins might self-associate to form a discrete fiber network for each chromatid. This might have the diffuse morphology of expanded scaffolds. Later, at metaphase, the scaffold could condense further (see Fig. 7), a process which might bring about the final stages of chromosome condensation. This postulated dynamic behavior of the scaffold proteins could be regulated in a cell-cycle-dependent manner via protein modification, as has been proposed for the components of the peripheral nuclear lamina (55). Such a model has the advantage that chromosome con-

densation is controlled by the self-assembly of a rather simple (at least at the level of protein composition) structure—the chromosome scaffold.

We would like to thank E. Boy de la Tour for advice and use of microscope facilities and J. Kistler, C. Lewis, and F. Keppel for their comments on the manuscript.

This work was supported by the Swiss National Science Foundation grant 3.621.80, and by the state of Geneva.

Received for publication 27 April 1982, and in revised form 27 September 1982.

REFERENCES

1. Igo-Kemenes, T., and H. G. Zachau. 1977. Domains in chromatin structure. *Cold Spring Harbor Symp. Quant. Biol.* 42:109–118.
2. Hyde, J. E. 1982. Expansion of chicken erythrocyte nuclei upon limited micrococcal nuclease digestion. *Exp. Cell Res.* 140:63–70.
3. Benyajati, C., and A. Worcel. 1976. Isolation, characterization, and structure of the folded interphase chromosome of *Drosophila melanogaster*. *Cell.* 9:393–407.
4. Cook, P. R., and I. A. Brazell. 1978. Spectrophotometric measurement of the binding of ethidium to superhelical DNA from cell nuclei. *Eur. J. Biochem.* 84:465–477.
5. Hartwig, M. 1978. Organization of mammalian chromosomal DNA: supercoiled and folder circular DNA subunits from interphase cell nuclei. *Acta Biol. Med. Ger.* 37:421–432.
6. Vogelstein, B., D. M. Pardoll, and D. S. Coffey. 1980. Supercoiled loops and eukaryotic DNA replication. *Cell.* 22:79–85.
7. Gall, J. G. 1955. Problems of structure and function in the amphibian oocyte nucleus. *Symp. Soc. Exp. Biol.* 9:358–370.
8. Callan, H. G. 1963. The nature of lampbrush chromosomes. *Int. Rev. Cytol.* 15:1–34.
9. Miller, O. L. 1965. Fine structure of lampbrush chromosomes. *Int. Symp.* on Genes and Chromosomes, Structure and Function. Natl. Cancer Inst. Monograph 8:79–99.
10. Gall, J. G. 1963. Chromosome fibers from an interphase nucleus. *Science (Wash. D. C.).* 139:120–121.
11. DuPraw, E. J. 1965. The organization of nuclei and chromosomes in honeybee embryonic cells. *Proc. Natl. Acad. Sci. U. S. A.* 53:161–168.
12. DuPraw, E. J. 1965. Macromolecular organization of nuclei and chromosomes: a folded fiber model based on whole-mount electron microscopy. *Nature (Lond.).* 206:338–343.
13. Bahr, G. F. 1970. Human chromosome fibers. Consideration of DNA-protein packing and of looping patterns. *Exp. Cell Res.* 62:39–49.
14. Ohnuki, Y. 1968. Structure of chromosomes. I. Morphological studies of the spiral structure of human somatic chromosomes. *Chromosoma (Berl.).* 25:402–428.
15. Utsumi, K. R., and T. Tanaka. 1975. Studies on the structure of chromosomes. I. The uncoiling of chromosomes revealed by treatment with hypotonic solution. *Cell Struct. Funct.* 1:93–99.
16. Ris, H. 1945. The structure of meiotic chromosomes in the grasshopper and its bearing on the nature of "chromomeres" and "lamp-brush chromosomes". *Biol. Bull.* 89:242–257.
17. Wray, W., and E. Stubblefield. 1970. A new method for the rapid isolation of chromosomes, mitotic apparatus, or nuclei from mammalian fibroblasts at near neutral pH. *Exp. Cell Res.* 59:469–478.
18. Stubblefield, E., and W. Wray. 1971. Architecture of the chinese hamster metaphase chromosome. *Chromosoma (Berl.).* 32:262–294.
19. Paulson, J. R., and U. K. Laemmli. 1977. The structure of histone-depleted chromosomes. *Cell.* 12:817–828.
20. Laemmli, U. K., S. M. Cheng, K. W. Adolph, J. R. Paulson, J. A. Brown, and W. R. Baumbach. 1978. Metaphase chromosome structure: the role of nonhistone proteins. *Cold Spring Harbor Symp. Quant. Biol.* 42:351–360.
21. Marsden, M. P. F., and U. K. Laemmli. 1979. Metaphase chromosome structure: evidence for a radial loop model. *Cell.* 17:849–858.
22. Rattner, J. B., M. Goldsmith, and B. A. Hamkalo. 1980. Chromatin organization during meiotic prophase of *Bombyx mori*. *Chromosoma (Berl.).* 79:215–224.
23. Rattner, J. B., M. Goldsmith, and B. A. Hamkalo. 1981. Chromatin organization during male meiosis in *Bombyx mori*. *Chromosoma (Berl.).* 82:341–351.
24. Adolph, K. W. 1980. Isolation and structural organization and human mitotic chromosomes. *Chromosoma (Berl.).* 76:23–33.
25. Adolph, K. W. 1981. A serial sectioning study of the structure of human mitotic chromosomes. *Eur. J. Cell Biol.* 24:146–153.
26. Bak, A. L., J. Zeuthen, and F. H. C. Crick. 1977. Higher-order structure of human mitotic chromosomes. *Proc. Natl. Acad. Sci. U. S. A.* 74:1595–1599.
27. Bak, A. L., and J. Zeuthen. 1978. Higher-order structure of mitotic chromosomes. *Cold Spring Harbor Symp. Quant. Biol.* 42:367–377.
28. Sedat, J., and L. Manuelidis. 1978. A direct approach to the structure of eukaryotic chromosomes. *Cold Spring Harbor Symp. Quant. Biol.* 42:331–350.
29. Adolph, K. W., S. M. Cheng, and U. K. Laemmli. 1977. Role of nonhistone proteins in metaphase chromosome structure. *Cell.* 12:805–816.
30. Adolph, K. W., S. M. Cheng, J. R. Paulson, and U. K. Laemmli. 1977. Isolation of a protein scaffold from mitotic HeLa cell chromosomes. *Proc. Natl. Acad. Sci. U. S. A.* 74:4937–4941.
31. Lebkowski, J. S., and U. K. Laemmli. 1982. Non-histone proteins and long-range organization of HeLa interphase DNA. *J. Mol. Biol.* 156:325–344.
32. Lewis, C. D., and U. K. Laemmli. 1982. Higher-order metaphase chromosome structure: evidence for metalloprotein interactions. *Cell.* 29:171–181.
33. Blumenthal, A. B., J. D. Dieden, L. N. Kapp, and J. W. Sedat. 1979. Rapid isolation of metaphase chromosomes containing high molecular weight DNA. *J. Cell Biol.* 81:255–259.
34. Kuo, M. T. 1982. Comparison of chromosomal structures isolated under different conditions. *Exp. Cell Res.* 138:221–229.
35. Lowry, O. H., H. J. Rosebrough, A. J. Farr, and R. J. Randall. 1951. Protein measurement with the Folin phenol reagent. *J. Biol. Chem.* 193:265–275.
36. Berlowitz, L., R. Kitchin, and D. Pallotta. 1972. Histones and RNA synthesis: selective binding of histones by a synthetic polyanion in calf thymus nuclei. *Biochem. Biophys. Acta.* 262:160–168.
37. Stein, A., J. P. Whitlock, Jr., and M. Bina. 1979. Acidic polypeptides can assemble both histones and chromatin in vitro at physiological ionic strength. *Proc. Natl. Acad. Sci. U. S. A.* 76:5000–5004.
38. Okada, T. A., and D. E. Comings. 1980. A search for protein cores in chromosomes: is the scaffold and artefact? *Am. J. Hum. Genet.* 32:814–832.
39. Hadlaczky, G., A. T. Sumner, and A. Ross. 1981. Protein-depleted chromosomes. II. Experiments concerning the reality of chromosome scaffolds. *Chromosoma (Berl.).* 81:557–567.
40. Markwell, M. A. K., S. M. Haas, H. L. L. Bieber, and N. E. Tolbert. 1979. A modification of the Lowry procedure to simplify protein determination in membrane and lipoprotein samples. *Anal. Biochem.* 87:206–210.
41. Hotchkiss, R. D. 1957. Methods for the characterization of nucleic acid. *In* Methods in Enzymolgy, Vol. 3. S. P. Colowick, and N. O. Kaplan, editors. Academic Press, NY. 710.
42. Labhardt, P., and T. Koller. 1981. Electron microscope preparation of rat liver chromatin by a modified Miller procedure. *Eur. J. Cell Biol.* 24:309–316.
43. Cole, A. 1967. Chromosome structure. *Theoretical Biophysics* 1:305–375.
44. Thoma, F., T. Koller, and A. Klug. 1979. Involvement of histone H1 in the organization of the nucleosome and of the salt-dependent superstructure of chromatin. *J. Cell Biol.* 83:403–427.
45. Finch, J. T., L. C. Lutter, D. Rhoades, R. S. Brown, B. Rushton, M. Levitt, and A. Klug. 1977. Structure of the nucleosome core particles of chromatin. *Nature (Lond.).* 269:29–36.
46. Hadlaczky, G., A. T. Sumner, and A. Ross. 1981. Protein-depleted chromosomes. I. Structure of isolated protein-depleted chromosomes. *Chromosoma (Berl.).* 81:537–555.
47. Miller, O. L., and B. R. Beatty. 1969. Visualization of nucleolar genes. *Science (Wash. D. C.).* 164:955–957.
48. Rattner, J. B., A. Branch, and B. A. Hamkalo. 1975. Higher order structure of metaphase chromosomes. I. The 250Å fiber. *Chromosoma (Berl.).* 69:363–372.
49. Dresser, M. E., and M. J. Moses. 1979. Silver staining of synaptonemal complexes for light and electron microscopy. *Exp. Cell Res.* 121:416–419.
50. Fletcher, J. M. 1979. Light microscope analysis of meiotic prophase chromosomes by silver staining. *Chromosoma (Berl.).* 72:241–248.
51. Pathak, S., and T. C. Hsu. 1979. Silver-stained structures in mammalian meiotic prophase. *Chromosoma (Berl.).* 70:195–203.
52. Howell, W. M., and T. C. Hsu. 1979. Chromosome core structure revealed by silver staining. *Chromosoma (Berl.).* 73:61–66.
53. Satya-Prakash, K. L., T. C. Hsu, and S. Pathak. 1980. Behavior of the chromosome core in mitosis and meiosis. *Chromosoma (Berl.).* 81:1–8.
54. Bloom, S. E., and C. Goodpasture. 1976. An improved technique for selective silver staining of nucleolar organizer regions in human chromosomes. *Hum. Genet.* 34:199–206.
55. Gerace, L., and G. Blobel. 1980. The nuclear envelope lamina is reversably depolymerized during mitosis. *Cell.* 19:277–287.